

# Combined VLBI- and X-ray Observations of Active Galactic Nuclei

M. Kadler<sup>1</sup>, E. Ros<sup>1</sup>, J. Kerp<sup>2</sup>, Y. Y. Kovalev<sup>3,4</sup>, and J. A. Zensus<sup>1</sup>

<sup>1</sup> Max-Planck-Institut für Radioastronomie, Auf dem Hügel 69, 53121 Bonn, Germany

<sup>2</sup> Radioastronomisches Institut der Universität Bonn, Auf dem Hügel 71, 53121 Bonn, Germany

<sup>3</sup> National Radio Astronomy Observatory, P.O. Box 2, Green Bank, WV 24944

<sup>4</sup> Astro Space Center of P. N. Lebedev Physical Institute, Profsoyuznaya 84/32, 117997 Moscow, Russia

**Abstract.** Compact radio cores in radio-loud active galactic nuclei (AGNs) are classical targets of Very-Long-Baseline interferometric (VLBI) research. Until today little has been known about their X-ray properties in comparison to radio-quiet AGNs. Here, we present results from a systematic X-ray spectral survey of radio-loud AGNs. This study is based on a statistically complete sample of regularly monitored compact, extragalactic radio jets from the VLBA 2 cm Survey and makes use of high-quality X-ray spectroscopic data from the archives of the X-ray observatories *ASCA*, *BeppoSax*, *CHANDRA*, and *XMM-Newton*. Combined VLBI and X-ray observations of AGNs can yield direct observational links between the central parsecs of extragalactic jets and dynamical processes within the accretion flows around supermassive black holes. It is essential to establish such links, which might have the power to attack the unsolved problem: “What makes an AGN radio-loud?” We present some early results from our survey project and report briefly on detailed studies of 0716+714, NGC 1052, and 3C 390.3.

## 1. Introduction

The question how powerful relativistic plasma jets are formed in the environment of supermassive black holes in active galactic nuclei (AGN) is a crucial one. Whilst a wealth of information about the jets themselves, in particular about their variable structure on parsec scales (e.g., Kellermann et al. 2004), can be obtained from VLBI, observational input that may lead to the disclosure of the fundamental difference between (jet-forming) radio-loud and (jet-suppressing) radio-quiet AGN is rare. Promising diagnostics of jet production are the accretion flows onto the central black holes. These accretion flows can be probed via X-ray spectroscopy, a technique which has dramatically benefitted from the advent of the new-generation X-ray telescopes *CHANDRA* and *XMM-Newton*. Their broad bandpasses, combined with the high sensitivity of *XMM-Newton* and the high angular resolution of *CHANDRA* have greatly improved our ability to identify the underlying physical processes of nuclear X-ray emission from AGN. Differences between the X-ray spectra of radio-loud and radio-quiet AGN may represent different physical properties of the accretion flows, dilution by an emission component directly associated with the jet, or even differences in the surrounding medium of their central engines.

Compared to radio-quiet AGN, little attention has been paid to radio-loud AGN in the X-ray band in the past. Sambruna et al. (1999; 2002) have investigated the X-ray spectra of 38 radio-loud AGN observed by *ASCA* and four sources observed by *RXTE*. Gambill et al. (2003) analyzed a sample of 17 radio-loud AGN observed with *CHANDRA*. These studies were based on the integrated radio emission measured by single-dish telescopes or biased towards the presence of prominent extended radio-jet structure. To approach the characteristic differences between both classes of objects, however, it is important to avoid confusion from considering extended radio emission that arises on kiloparsec scales. In the most extreme case,

emission from extended radio lobes – millions of light years away from the central engine – might still make a galaxy radio-loud when the nuclear jet-production has already been switched off for ages.

The radio emission of core-dominated radio-loud AGN is heavily affected by relativistic beaming effects due to large jet velocities and typically small angles to the line of sight. Thus, it is essential to combine X-ray studies of core-dominated radio-loud AGN with VLBI monitoring observations of their parsec-scale radio jets to constrain the jet-system properties. Ideally, this combination promises to disentangle the contributions of “Seyfert-like” accretion-flow related emission and jet-associated (e.g., synchrotron self-Compton) emission in core-dominated radio-loud AGN. Ultimately, this approach might allow the fundamental question to be addressed: “What makes AGN radio-loud?”

## 2. An X-ray spectral survey of radio-loud core-dominated AGN

Our sample is based on the statistically complete MOJAVE sample (e.g., Ros 2003; M. L. Lister et al., in prep.), a Very Long Baseline Array (VLBA) monitored sample of the 133 brightest core-dominated radio-loud AGN in the northern sky (see <http://www.physics.purdue.edu/astro/MOJAVE/>). The kinematics of individual features within the jet structures of these sources are being monitored since 1994 within the scope of the VLBA 2 cm Survey (see e.g., Ros, these proceedings). We analyze the X-ray spectra of radio-loud core-dominated AGN from the MOJAVE sample by making use of the publicly available archival data from the telescopes *ASCA*, *BeppoSax*, *CHANDRA*, and *XMM-Newton*. Table 1 gives the 55 resulting sources of our sample (the “2 cm-X-Sample” from here on).

**Table 1.** The 2cm-X-Sample

Source <sup>a</sup>	Alt. Name	C <sup>1</sup>	X <sup>2</sup>	A <sup>3</sup>	B <sup>4</sup>	Source <sup>a</sup>	Alt. Name	C <sup>1</sup>	X <sup>2</sup>	A <sup>3</sup>	B <sup>4</sup>
0007+106	III Zw 2	✓	✓	✓		1228+126	M 87	✓	✓	✓	✓
0048-097	OB -080			✓		1253-055	3C 279	✓		✓	✓
0202+149	4C 15.05		✓			1308+326	OP +313		✓	✓	
0234+285	CTD 20			✓		1334-127	OP -158.3			✓	
0235+164	OD +160	✓	✓	✓		1413+135	OQ +122			✓	
0238-084	NGC 1052	✓	✓	✓		1458+718	3C 309.1	✓			
0316+413	3C 84	✓	✓	✓		1502+106	4C 10.39		✓		
0333+321	NRAO 140		✓	✓		1510-089	OR -017	✓		✓	✓
0415+379	3C 111	✓	✓	✓		1611+343	DA 406			✓	✓
0420-014	OA +129		✓	✓		1633+382	4C 38.41			✓	
0430+052	3C 120	✓	✓	✓		1641+399	3C 345	✓		✓	
0458-020	DA 157	✓				1655+077	OS +092	✓			
0528+134	OG +147		✓	✓		1741-038	OT -068			✓	
0605-085	OH -010	✓				1749+096	4C 09.57			✓	
0716+714			✓	✓		1803+784				✓	
0735+178	DA 237		✓			1823+568	4C 56.27			✓	
0736+017			✓	✓		1828+487	3C 380	✓			
0738+313	OI +363	✓	✓			1928+738	4C 73.18	✓		✓	✓
0827+243		✓				1936-155				✓	
0836+710	4C 71.07	✓	✓	✓		1957+405	Cyg A	✓		✓	✓
0851+202	OJ +287		✓	✓		2134+004	DA 553			✓	
0923+392	4C 39.25	✓		✓		2145+067				✓	
1038+064	4C 06.41	✓	✓			2200+420	BL Lac	✓		✓	✓
1055+018	4C 01.28	✓				2223-052	3C 446			✓	✓
1127-145	OM -146	✓	✓	✓		2230+114	CTA 102			✓	✓
1156+295	4C 29.45	✓				2243-123	OY -176			✓	
1222+216		✓		✓		2251+158	3C 454.3	✓		✓	
1226+023	3C 273	✓	✓	✓							

<sup>a</sup> B 1950.0 coordinates; <sup>1</sup> Archival *CHANDRA* data; <sup>2</sup> Archival *XMM-Newton* data; <sup>3</sup> Archival *ASCA* data; <sup>4</sup> Archival *BeppoSax* data

Figure 1 (top panels) shows the distribution of mean VLBI radio fluxes for the 2 cm-X-Sample in comparison to the distribution for the whole MOJAVE sample. In the middle panels of Fig. 1 the comparison of the source compactness (i.e., unresolved flux on the longest VLBA baselines at 15 GHz divided by the total recovered VLBI flux) is shown. These distributions for the whole MOJAVE sample are analyzed in detail in Y. Y. Kovalev et al. (in prep.). As for the MOJAVE sample, the peak of the VLBI flux distribution for the 2 cm-X-Sample reflects the selection limit while the low flux density wing reflects the variable nature of AGN. The distribution of the mean source compactness shows, in agreement with expectations from unification models of radio galaxies, quasars and BL Lacs, the rising compactness from galaxies to quasars to BL Lacs for both samples. The bottom panels of Fig. 1 display the distributions for the 2 cm-X-Sample and the whole MOJAVE sample of the apparent linear velocity of the brightest component in each source with well determined kinematics. The apparent bimodality of speeds for the full 2 cm sample and the MOJAVE sample reported in Kellermann et al. (2004) is present also for the 2 cm-X-Sample, with a minimum (most pronounced for the quasar distribution) around  $\beta_{\text{app}} \sim 8$ .

A Kolmogorov-Smirnov test does not reveal any significant differences between both samples, so that we consider the 2 cm-X-Sample to be representative of the statistically complete MOJAVE sample. It thus provides a firm basis for sta-

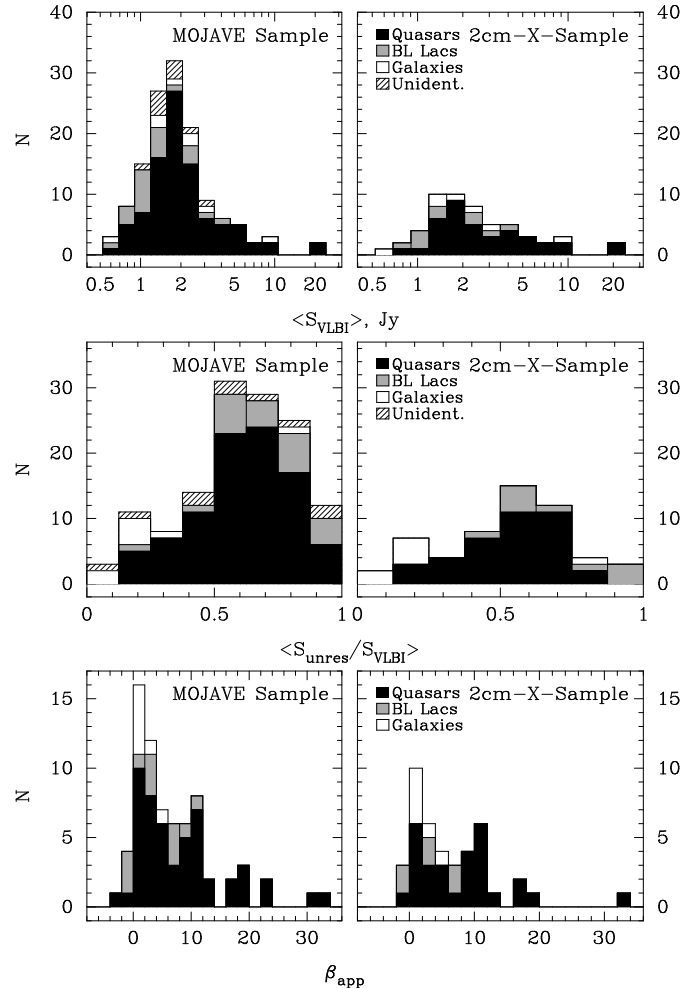


**Fig. 1.** Distribution of the statistically complete MOJAVE sample and the 2 cm-X-sample observed at X-rays spectroscopically over the mean total flux density  $S_{\text{VLBI}}$  observed by the VLBA (top), the mean compactness index  $S_{\text{unres}}/S_{\text{VLBI}}$  (middle), and the apparent linear velocity  $\beta = v/c$  of well determined jet components. In all histograms the sources are divided by optical classification into quasars, BL Lac objects and galaxies.

tistical investigations of core-dominated radio-loud AGN. The statistical analysis of our sample (e.g., the mean photon index, absorbing column density, luminosity ratios, and broadband spectral energy distributions) and the comparison to radio-quiet AGN and the radio-loud AGN samples of Sambruna et al. (1999; 2002) and Gambill et al. (2003) will be presented by M. Kadler et al. (in prep.).

### 3. Radio and X-ray studies of individual sources

Several individual source studies already have been conducted connected to this survey project. We present here three cases that are of special interest. Another example is the multi-waveband analysis from subparsec to megaparsec scales of the superluminal quasar 3C 454.3, which is presented by Pagels et al. (these proceedings).

0716+714: The BL Lac source 0716+714 was contained in-

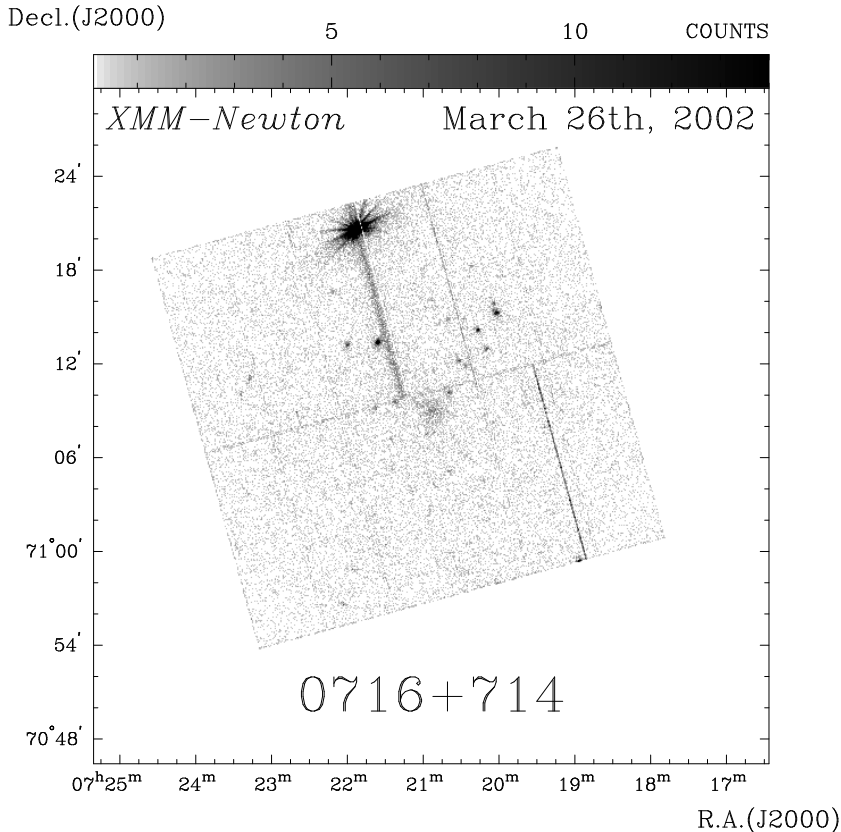


**Fig. 2.** Raw photon image of the *XMM-Newton* pn-chip during the 6.6 ksec observation of the galaxy cluster C0720.8+7109 in March 2002. 0716+714 is visible as a bright point source close to the top edge of the image.

side the field of view of three *XMM-Newton* observations of the galaxy cluster C0720.8+7109 (see Fig. 2). The X-ray spectral analysis reveals a variable composition of synchrotron and inverse Compton emission and strong short-term variability with energy dependent time lags of soft and hard photons (Kadler et al. 2004c). So far, 0716+714 has withstood all attempts to determine its redshift directly. Only indirectly a limit of  $z > 0.3$  has been derived from the non-detection of the optical host galaxy (Wagner et al. 1996). The *XMM-Newton* spectrum shows evidence for line emission at  $\sim 5.8$  keV in one epoch. If interpreted as iron  $K\alpha$  emission emitted from material at rest in the quasars frame, this implies a surprisingly small redshift of 0716+714 of only  $z = 0.1$ . Additional observations with *XMM-Newton* and/or *Astro-E2* are necessary to solve this issue.

**NGC 1052:** A high angular resolution snapshot *CHANDRA* observation of this low-luminosity AGN revealed the origin of its soft X-ray excess emission. Soft thermal plasma emission is produced in an extended region around the active nucleus, most likely originating from jet-driven shock heating of the host galaxies interstellar medium (Kadler et al. 2004a). The highest signal-to-noise X-ray spectrum of NGC 1052 comes from a 13 ksec *XMM-Newton* observation, disclosing the presence of a highly relativistic broad iron line (Kadler et al. 2004b). The variable broad iron line and the prominent nuclear radio-jet structure of NGC 1052 might provide a direct observational probe of jet-disk coupling in an active galaxy.

**3C 390.3<sup>1</sup>:** To our knowledge, there is only one source apart from NGC 1052 for which the profile of a broad X-ray spec-

tral feature could be significantly better approximated by a relativistic iron-line model rather than by a narrow or broad Gaussian line component: the broad-line radio galaxy 3C 390.3 (Sambruna et al. 1999).

Here, we report the highest signal-to-noise X-ray spectrum of 3C 390.3 so far obtained, from a 35 ksec *CHANDRA* observation. In Fig. 3, we show the X-ray spectrum of 3C 390.3 together with its rich large-scale X-ray brightness distribution. Several knots in the north-west and south-east of the nucleus can be found, some of them corresponding to knots or hot-spots in the radio structure. The detailed analysis of these data will be presented elsewhere. We find a comparably flat X-ray spectrum ( $\Gamma \sim 1.4$  for a simple absorbed-power-law fit), which is best approximated by either an absorbed broken power law or a high-energy-reflected power-law spectrum with an intrinsic photon index of 1.6 to 1.7 in both cases. The residuals (bottom panel at the top right illustration in Fig. 3) show no obvious evidence for excess iron-line emission. For both models the fit does not improve significantly when an additional line component is added to the model. Thus, the *CHANDRA* data do not support the relativistic iron-line scenario for 3C 390.3.

#### 4. Radio-quiet AGN with broad iron lines

Apart from NGC 1052, there are a number of confirmed and disputed broad-iron-line detections in radio-quiet sources, namely Seyfert 1 galaxies. Despite their weak radio emission, Seyfert galaxies often harbor compact radio cores (e.g.,

<sup>1</sup> 3C 390.3 is part of the VLBA 2 cm Survey sample but does not belong to the MOJAVE sample and is not considered for our statistical

analysis. We present its X-ray spectrum here because of its relevance for the study of broad iron line emission from radio-loud AGN.

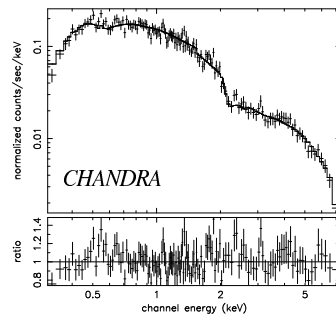
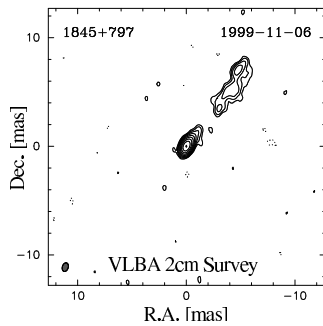
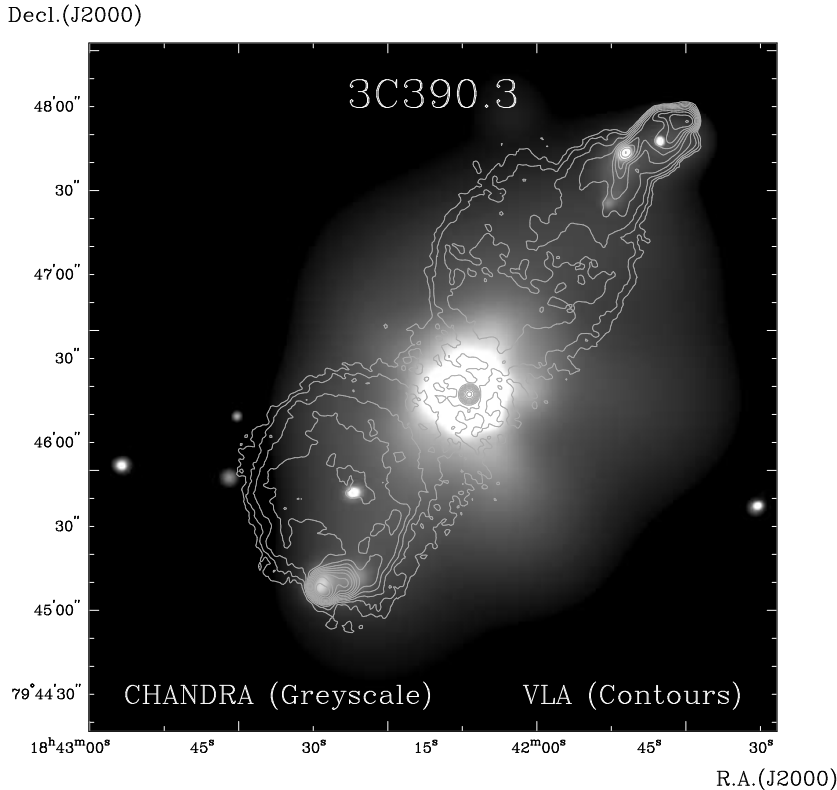


**Fig. 3.** Top: The kpc-scale radio- and X-ray structure of 3C 390.3. The 1.6 GHz radio jet (taken from the NED archive and previously published by Leahy & Perley 1991) is superimposed on the integrated 0.2 keV to 8 keV X-ray brightness distribution from a 35 ksec *CHANDRA* observation (PI: S. Wagner). Bottom left: The milliarcsecond structure of the nuclear radio jet in November 1999. Bottom right: X-ray spectrum of 3C 390.3 and residuals after subtracting a high-energy-reflected power-law spectrum model.

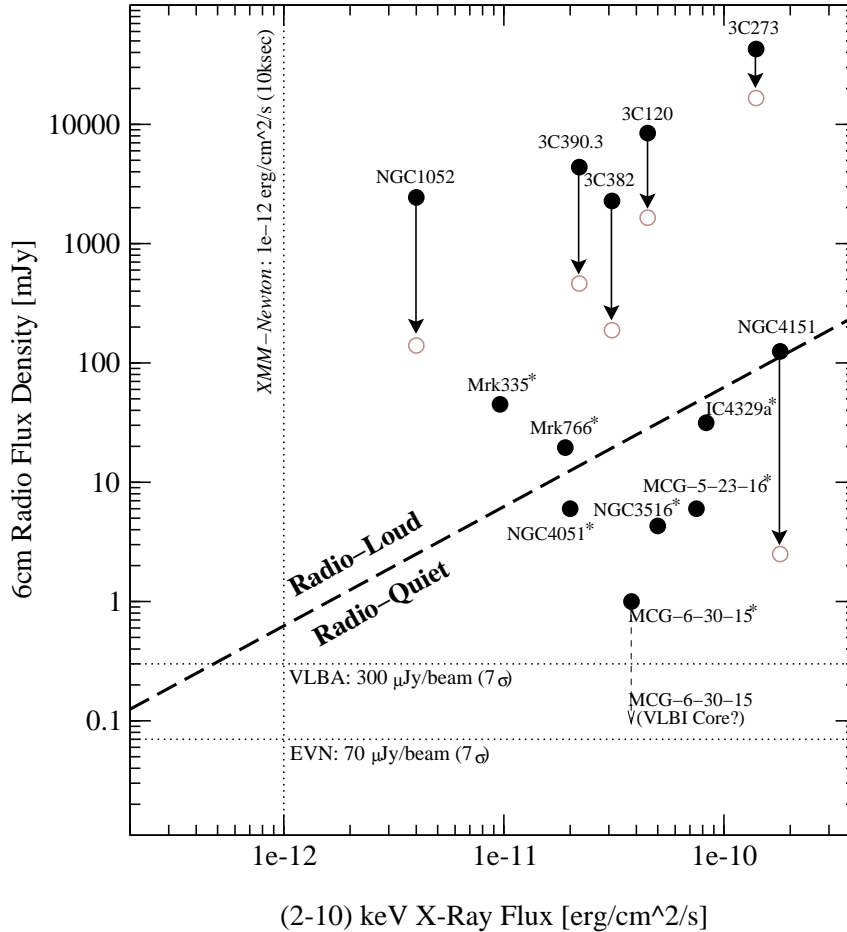
Middelberg et al. 2004). In some cases, VLBI observations reveal a parsec-scale jet structure in these sources. Such compact radio cores in radio-quiet broad-iron-line systems are potentially attractive targets for high-sensitivity VLBI observations because of their well studied accretion-disk dynamics.

Figure 4 displays the positions in the radio-flux-density vs. X-ray-flux plane<sup>2</sup> of the undisputed broad-iron-line Seyfert galaxies MCG-6-30-15 (Fabian et al. 2002; Wilms et al. 2001), MCG-5-23-16 (Dewangan et al. 2003), NGC 3516 (Turner et al. 2002), Mrk 335 (Gondoin et al. 2002), and Mrk 766 (Pounds et al. 2003). In addition, the sources IC 4329a (Gondoin et al. 2001; Mc Kernan & Yaqoob 2004), and NGC 4151 (Schurch et al. 2003) are shown, in which *ASCA* detected broad iron lines which could not be confirmed by *XMM-Newton* or are disputed. Finally, the radio-loud sources 3C 120 (Ogle et al. 2004), 3C 273 (Page et al. 2004; Yaqoob & Serlemitsos 2000), 3C 382 (Sambruna et al. 1999), 3C 390.3 (Sambruna et al. 1999

and this work), and NGC 1052 (Kadler et al. 2004b) are also plotted. Figure 4 shows that not only the radio-loud AGN are accessible by VLBI, but also the so-called radio-quiet Seyfert galaxies. In particular, the EVN with its large antennas provides enough sensitivity to image, e.g., the parsec-scale structure of the possibly most interesting broad-iron-line Seyfert galaxy MCG-6-30-15, given that it harbors a compact nucleus on milliarcsecond scales.

*Acknowledgements.* M.K. was supported for this research through a stipend from the International Max Planck Research School (IMPRS) for Radio and Infrared Astronomy at the University of Bonn. Y.Y.K. is a Jansky Fellow. Part of this work was done within the framework of the VLBA 2cm Survey collaboration (see <http://www.cv.nrao.edu/2cmSurvey>). This research was supported by the European Commission’s I3 Programme “RADIONET”, under contract No. 505818. The VLBA is an instrument of the U.S.A. National Radio Astronomy Observatory, which is a facility of the National Science Foundation, operated under cooperative agreement by Associated Universities, Inc. X-ray archival data are made available from the High Energy Astrophysics Science Archive Research Center (HEASARC), provided by NASA’s Goddard Space Flight Center.

<sup>2</sup> Fluxes are taken from Fomalont et al. (2000), Giovannini et al. (2001), Gregory & Condon (1991), Morganti et al. (1999), Rush et al. (1996), Sambruna et al. (1999), Stickel et al. (1994), Ulvestad & Wilson (1984), and the HEASARC website.



**Fig. 4.** Radio and X-ray fluxes of confirmed and disputed broad-iron-line AGN systems. The radio-loud/quiet dividing line follows the definition of Terashima & Wilson (2003). The arrows indicate the range from integrated (single-dish: filled circles) flux density to VLBI-core flux density (open circles). Only integrated (VLA) flux densities are given for the radio-quiet objects (marked by an asterisk). The arrow for MCG-6-30-15 indicates that the flux density of the compact core component might be well below the integrated (although compact on VLA scales) value. Approximate sensitivity limits for the EVN, the VLBA, and *XMM-Newton* are shown. The EVN and VLBA limits correspond to deep 5 hour integrations with 1024 Mbps (EVN) and 256 Mbps and a  $7\sigma$  detection of an unresolved image feature. The *XMM-Newton* limit at  $10^{-12}$  erg  $\text{cm}^{-2}$   $\text{s}^{-1}$  corresponds to the minimal source flux for which a 1000-photon spectrum can be obtained in a 10 ksec pointing.

## References

- Dewangan, G. C., Griffiths, R. E., & Schurch, N. J. 2003, *ApJ*, 592, 52
- Fabian, A. C., Ballantyne, D. R., Merloni, A., et al. 2002, *MNRAS*, 331, L35
- Fomalont, E. B., Frey, S., Paragi, Z., et al. 2000, *ApJS*, 131, 95
- Gambill, J. K., Sambruna, R. M., Chartas, G., et al. 2003, *A&A*, 401, 505
- Giovannini, G., Cotton, W. D., Feretti, L., Lara, L., & Venturi, T. 2001, *ApJ*, 552, 508
- Gondoin, P., Barr, P., Lumb, D., et al. 2001, *A&A*, 378, 806
- Gondoin, P., Orr, A., Lumb, D., & Santos-Lleó, M. 2002, *A&A*, 388, 74
- Gregory, P. C., & Condon, J. J. 1991, *ApJS*, 75, 1011
- Kadler, M., Kerp, J., Ros, E., et al. 2004a, *A&A*, 420, 467
- Kadler, M., Ros, E., Weaver, K. A., Kerp, J., Zensus, J. A. 2004b, *BAAS* 36, No. 2, 823
- Kadler, M., Kerp, J., & Krichbaum, T. P. 2004c, *A&A*, submitted
- Kellermann, K. I., Sramek, R., Schmidt, M., Shaffer, D. B., & Green, R. 1989, *ApJ*, 98, 1195
- Kellermann, K. I., Lister, M. L., Homan, D. C., et al. 2004, *ApJ*, 609, 539
- Leahy, J. P. & Perley, R. A. 1991, *ApJ*, 102, 537
- McKernan, B. & Yaqoob, T. 2004, *ApJ*, 608, 157
- Middelberg, E., Roy, A. L., Nagar, N. M., et al. 2004, *A&A*, 417, 925
- Morganti, R., Tsvetanov, Z. I., Gallimore, J., & Allen, M. G. 1999, *A&AS*, 137, 457
- Ogle, P. M., Davis, S. W., Antonucci, R. R. J., et al. 2004, *BAAS* 36, No. 2, 766
- Page, K. L., Turner, M. J. L., Done, C., et al. 2004, *MNRAS*, 349, 57
- Pounds, K. A., Reeves, J. N., Page, K. L., Wynn, G. A., & O'Brien, P. T. 2003, *MNRAS*, 342, 1147
- Ros, E. 2003, in *Highlights in Spanish Astrophysics III*, J. Gallego, J. Zamorano, N. Cardiel (eds.), Kluwer Academic Publishers, p.235
- Rush, B., Malkan, M. A., & Edelson, R. A. 1996, *ApJ*, 473, 130
- Sambruna, R. M., Eracleous, M., & Mushotzky, R. F. 1999, *ApJ*, 526, 60
- Sambruna, R. M., Eracleous, M., & Mushotzky, R. F. 2002, *New Astron. Rev.*, 46, 215
- Schurch, N. J., Warwick, R. S., Griffiths, R. E., & Sembay, S. 2003, *MNRAS*, 345, 423
- Stickel, M., Meisenheimer, K., & Kühr, H. 1994, *A&AS*, 105, 211
- Terashima, Y., & Wilson, A. S. 2003, *ApJ*, 583, 145
- Turner, T. J., Mushotzky, R. F., Yaqoob, T. et al. 2002, *ApJ*, 574, L123
- Ulvestad, J. S., & Wilson, A. S. 1984, *ApJ*, 285, 439
- Wagner, S. J., Witzel, A., Heidt, J., et al. 1996, *AJ*, 111, 2187
- Wilms, J., Reynolds, C. S., Begelman, M. C., et al. 2001, *MNRAS*, 328, L27
- Yaqoob, T., & Serlemitsos, P. 2000, *ApJ*, 544, L95